DOI: 10.1002/ejic.200800691

Structural and Spectroscopic Properties of New Copper(I) Complexes with 1,1,1-Tris(diphenylphosphanylmethyl)ethane and Heterocyclic Thiolates

Paraskevas Aslanidis,*[a] Philip J. Cox,[b] Konstantinos Kapetangiannis,[a] and Athanassios C. Tsipis*[c]

Keywords: Copper(I) complexes / Triphos / Heterocyclic thiolates / Luminescence / TD-DFT calculations

Reactions of copper(I) halides with 1,1,1-tris(diphenylphosphanylmethyl)ethane (triphos) in 1:1 molar ratio afforded mononuclear complexes of the type [CuX(triphos)] which on further treatment with one equivalent of the potassium thiolate salt of a heterocyclic thione gave rise to the formation of mixed-ligand complexes of the formula [Cu(κ^3-triphos)(κ^1-thiolate)]. The molecular structures of [Cu(κ^3-triphos)(κ^1-py2S)]·C_2H_5OH (**1**) and [Cu(κ^3-triphos)(κ^1-pymt)] (**2**) have been established by single-crystal X-ray diffraction. The complexes adopt a rigid distorted tetrahedral geometry with the phosphane ligand acting in a tridentate chelating mode. The complexes are strongly luminescent in solution and in the solid state. The spectroscopic and electronic properties of the new copper(I) complexes have been computed by electronic structure computational techniques (TD-DFT calculations), that contribute to the assignments of electronic spectra. The high-energy absorptions in the absorption spectra of complexes **1** and **2**, ranging from 210 to 270 nm, are assigned to MLCT/LLCT transitions and the same also holds true for the low-energy absorptions found in the range 280 to 300 nm. In the lowest triplet excited state, T_1, involved in the emission in the 456–502 nm range, the spin density is delocalized over the entire nuclear framework.

Introduction

Transition metal coordination compounds of polyphosphane ligands have been studied intensively over the past three decades for their potential applications as catalysts in several homogeneous catalytic reactions.[1] In this respect, particular interest has been devoted to the complexes of a sub-class of polyphosphane ligands called tripodal triphosphanes, among which the most extensively studied is 1,1,1-tris(diphenylphosphanylmethyl)ethane (triphos).[2] Although much work has been carried out on the coordination compounds of triphos of a variety of transition metals, its copper(I) coordination chemistry remained practically undeveloped, with the related reported structures being actually limited to the two simple halide monomeric complexes [CuX(κ^3-triphos)] (X = Cl, Br)[3,4] and to a few organo-copper(I) compounds, such as [CuPh(κ^3-triphos)][5] and [Cu(μ-CCPh)(κ^3-triphos)]$_2$.[6]

In previous work we explored the molecular architectures realized by thione-ligated copper(I) halide complexes containing tertiary arylphosphanes as bulky co-ligands.[7] Specifically, attempts have been made to decipher the interplay between steric and electronic properties of the ligands employed on the coordination number and nuclearity of the complexes obtained. Considering that the steric profile and the geometrical features of the mono- and bidentate phosphanes used as co-ligands so far play a key role in determining the intriguing, often unexpected geometries observed, we thought it would be advisable to further extend our investigations including polydentate phosphane ligands, such as with the triphos ligand. Accordingly, in the present study we exploited the structural, spectroscopic (luminescent), bonding and electronic properties of some mixed-ligand copper(I) complexes formulated as [Cu(κ^3-triphos)(thiolate)], using both experimental and computational (DFT and TD-DFT) methodologies in conjunction with single-crystal X-ray studies for two of them. Furthermore inspired by a recent theoretical study on the luminescence of four [Cu(κ^3-triphos)X] derivatives,[8] we instigated to further explore the relationship between structure and luminescence and evaluate the impact of the thiolate ligand on the luminescence properties of the new copper(I) complexes.

[a] Aristotle University of Thessaloniki, Faculty of Chemistry, Inorganic Chemistry Laboratory,
P. O. Box 135, 54124 Thessaloniki, Greece
E-mail: aslanidi@chem.auth.gr
[b] School of Pharmacy, The Robert Gordon University,
Schoolhill, Aberdeen AB10 1FR, Scotland
E-mail: p.j.cox@rgu.ac.uk
[c] Section of Inorganic and Analytical Chemistry, Department of Chemistry, University of Ioannina,
45110 Ioannina, Greece
E-mail: attsipis@cc.uoi.gr

Supporting information for this article is available on the WWW under http://www.eurjic.org or from the author.

Results and Discussion

Preparative Aspects

The ability of 1,1,1-tris(diphenylphosphanylmethyl)ethane, $(Ph_2PCH_2)_3CMe$, (triphos) to preferably act as a tripodal ligand generating mononuclear four-coordinate copper(I) halide complexes is well known.[4] Having this in mind, we decided to approach the desired mononuclear mixed-ligand complexes starting from copper halides to ensure that coordination of triphos takes place in the established manner. On the other hand, thiolates instead of neutral thiones have been chosen to smoothly substitute the halide ligands. Along this line, the desired complex retaining its nuclearity and the geometry around copper has been successfully synthesized. Indeed, formation of the complexes under investigation was achieved by treatment of an acetonitrile suspension of CuBr with the equimolar quantity of triphos followed by the addition of 1 equiv. of potassium thiolate obtained by deprotonation of the parent heterocyclic thione with KOH in ethanol. This one-top two-step synthetic procedure proved, however, to be of limited applicability, as the microcrystalline or powdery solids obtained were found to correspond to the desired pure compounds only in a few cases. In particular, pyridine-2-thiolate (py2S$^-$), pyrimidine-2-thiolate (pymt$^-$), 4,6-methyl-pyrimidine-2-thiolate (dmpymt$^-$), 3,4,5,6-tetrahydro-pyrimidine-2-thiolate (tHpymt$^-$) and 4-methyl-5-trifluoromethyl-4*H*-1,2,4-triazoline-3(2*H*)-thiolate (mftzt$^-$) (Scheme 1) yielded small amounts of yellowish to orange crystals, which could be satisfactory defined as compounds **1**–**5** respectively, but only intractable materials were obtained for a number of other thiolates employed. Attempts to obtain the complexes by direct reaction of [Cu(κ^3-triphos)]NO_3 with the neutral thione ligands were not successful.

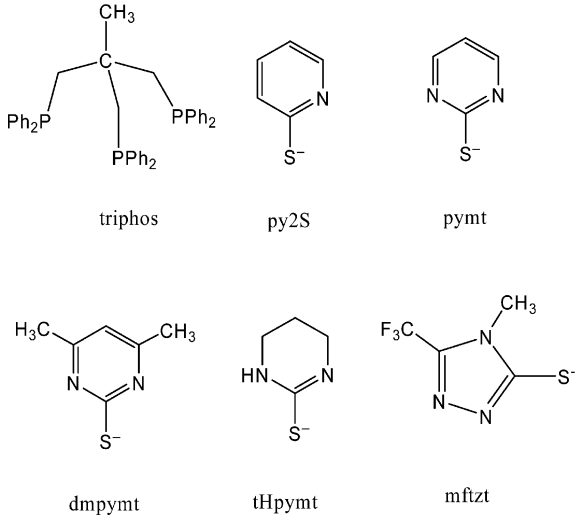

Scheme 1. The phosphane and the heterocyclic thiolates used as ligands along with their abbreviations.

All prepared compounds are air stable diamagnetic solids, soluble in chloroform and dichloromethane and moderately soluble in acetonitrile and acetone. Their solutions in common organic solvents are non-conducting. All synthesized complexes were characterized by elemental analyses and IR and ^{1}H NMR spectra. The molecular structures of [Cu(κ^3-triphos)(py2S)] (**1**) and [Cu(κ^3-triphos)(pymt)] (**2**) were determined by X-ray crystallographic analysis.

Spectroscopy

The IR spectra of complexes **1**–**5**, recorded in the range 4000–250 cm^{-1} display strong vibrational bands due to the phosphane ligand, which remain practically unshifted upon coordination. In addition, the spectra contain the expected characteristic "thioamide bands",[9] with shifts due to coordination indicative of an exclusive S-coordination mode.

The electronic absorption spectra recorded in dichloromethane at room temperature, show two intense bands with maxima in the 245–260 nm and 290–300 nm regions.

Compounds **1**–**5** exhibit an intense blue-green emission with λ_{max} values of the broad bands in the 456–502 nm range when excited at λ = 300 nm at room temperature in the solid state, while [CuBr(κ^3-triphos)] emits at λ_{max} = 463 nm. The absorption and emission data of the complexes under investigation are summarized in Table 1, and a representative absorption and emission spectrum of compound **1** is shown in Figure 1 (relevant excitation spectra of complexes **1**–**5** are given in Figure S1).

Table 1. Absorption and emission maxima of [Cu(κ^3-triphos)(thiolate)] complexes at room temperature.

Compound	λ_{max} [nm][a]	λ_{em} [nm][b]
[Cu(κ^3-triphos)(κ^1-py2S)] (**1**)	244, 291	502
[Cu(κ^3-triphos)(κ^1-pymt)] (**2**)	238, 296	469
[Cu(κ^3-triphos)(κ^1-dmpymt)] (**3**)	258, 293	459
[Cu(κ^3-triphos)(κ^1-tHpymt)] (**4**)	263, 298	456
[Cu(κ^3-triphos)(κ^1-mftzt)] (**5**)	241, 288	460

[a] Solution in CH_2Cl_2. [b] Solid state.

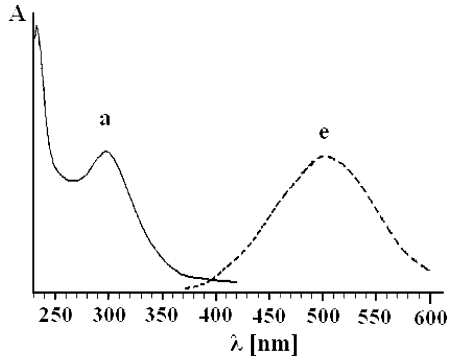

Figure 1. Electronic absorption (a) and emission (e) spectrum of [Cu(κ^3-triphos)(py2S)] (**1**) at room temperature. Absorption: 10^{-4} M in CH_2Cl_2, 1-cm cell. Emission: solid, λ_{exc} = 300 nm.

Various copper(I) phosphane complexes are luminescent in the solid state at room temperature, and in many cases the luminescence is found to be a phosphorescence.[10] Although the nature of the emissive excited states of these compounds has not been yet definitively clarified recent

TD-DFT calculations on some related complexes[8] showed the luminescence to have mixed character between metal–ligand charge transfer (MLCT) of the type $Cu^{I} \rightarrow \pi^{*}(PPh_2)$ and ligand–ligand charge transfer (LLCT), and this applies definitively also to the compounds under investigation, as supported by the TD-DFT calculations discussed below.

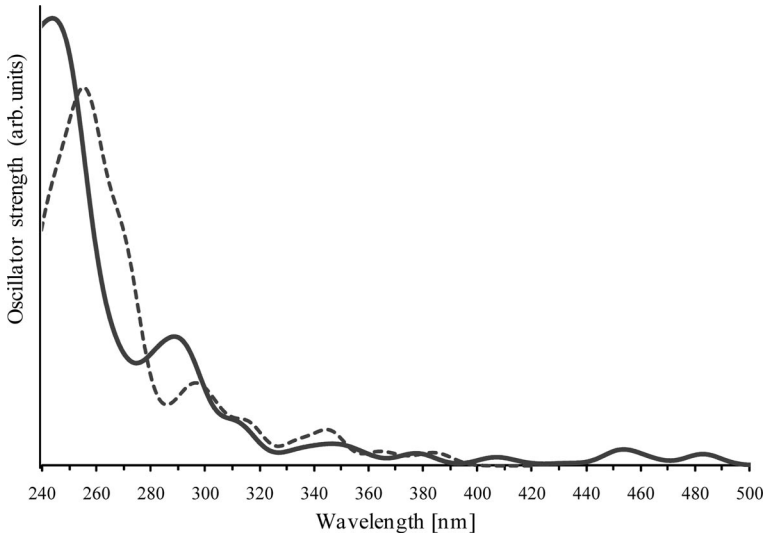

Figure 2. Absorption spectra of complexes **1** (solid line) and **2** (dashed line) simulated at the SAOP/TZP level in the gas phase (band width of 15 nm).

Table 2. Principal singlet-singlet optical transitions ($f > 0.01$) for the absorptions of complexes **1** and **2**, calculated in the gas phase using the SAOP/TZP method.

Excitation (% composition)	E [eV]	λ [nm]	OS, f
Complex **1**			
H-3→L (47.2%), H→L+12 (41.2%)	4.203	295	0.018
H-3→L (43.0%), H→L+12 (49.3%)	4.232	293	0.012
H→L+1 (78.5%)	4.350	285	0.011
H→L+3 (59.8%), H-4→L+2 (18.1%)	4.381	283	0.015
H-3→L+6 (43.7%), H-4→L+5 (33.7%)	4.769	260	0.012
H-4→L+6 (33.7%), H-4→L+5 (18.3%)	4.901	253	0.031
H-3→L+7 (80.4%)	4.940	251	0.017
H→L+15 (33.0%), H-3→L+8 (32.8%)	4.959	250	0.047
H-3→L+8 (63.3%)	5.020	247	0.054
H→L+16 (32.1%), H-3→L+9 (30.6%)	5.166	240	0.045
H→L+16 (37.8%), H-4→L+9 (19.1%)	5.209	238	0.071
H-4→L+9 (76.5%)	5.231	237	0.014
H-3→L+11 (39.1%), H-4→L+10 (35.1%)	5.391	230	0.017
H→L+19 (47.7%), H-1→L+13 (43.8%)	5.486	226	0.047
H→L+19 (51.6%), H-1→L+13 (36.1%)	5.510	225	0.065
H-3→L+12 (65.6%)	5.687	218	0.044
Complex **2**			
H-1→L+5 (87.3%)	4.168	297	0.010
H-2→L+4 (89.5%)	4.473	277	0.012
H-2→L+5 (48.9%), H-3→L+1 (15.3%), H-1→L+10 (14.8%)	4.580	271	0.019
H-3→L+1 (33.1%), H-2→L+5 (28.6%), H-3→L (25.5%)	4.588	270	0.011
H-2→L+6 (52.3%), H-1→L+10 (36.5%)	4.615	269	0.015
H-1→L+10 (46.4%), H-2→L+6 (39.8%)	4.628	268	0.018
H-1→L+12 (56.6%), H-2→L+7 (27%)	4.742	261	0.020
H-2→L+8 (39.2%), H→L+13 (22.7%), H-1→L+13 (19.5%)	4.815	257	0.051
H-2→L+8 (54.7%), H→L+13 (16%)	4.827	257	0.027
H-3→L+4 (86.7%)	4.898	253	0.019
H-4→L+2 (38.5%), H-4→L (17.8%)	4.946	251	0.012
H-3→L+5 (69.9%)	4.968	250	0.015
H-2→L+10 (90.6%)	5.011	247	0.013
H-3→L+6 (85.1%)	5.068	245	0.026
H-2→L+12 (86.9%)	5.131	242	0.019
H-3→L+7 (87.8%)	5.170	240	0.017

TD-DFT Simulated Absorption Spectra

The absorption spectra of complexes **1** and **2**, simulated using TD-DFT calculations in the gas-phase, are given in Figure 2. The TD-DFT principal singlet-singlet electronic transitions, excitation energies and oscillator strengths are compiled in Table 2. An orbital energy level diagram of the molecular orbitals involved in some of the most intense spin-allowed transitions is given in Figure 3 (the 3D contour plots of all molecular orbitals involved in the electronic transitions in the simulated absorption spectra of complexes **1** and **2** are depicted in Figures S2 and S3 of the Supporting Information).

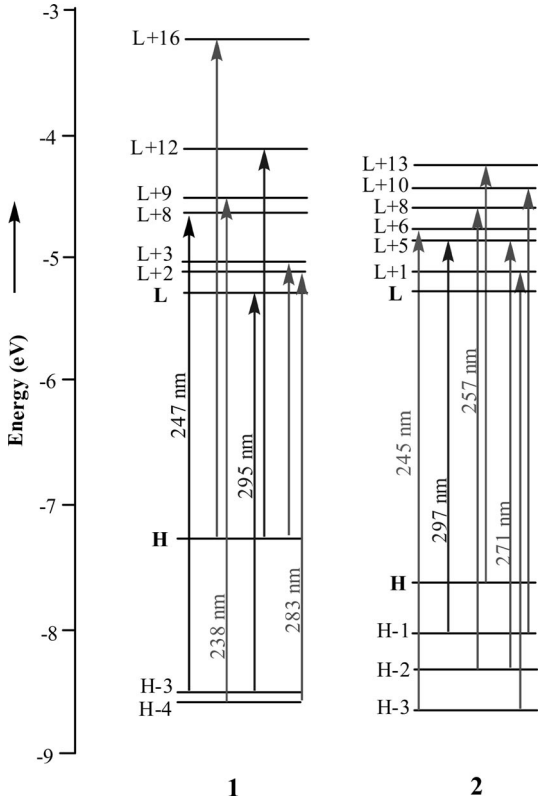

Figure 3. Orbital energy level diagrams of the molecular orbitals involved in some of the most intense spin-allowed electronic transitions for complexes **1** and **2** calculated by TD-DFT at the SAOP/TZP level.

The calculated absorption spectrum of complex **1** showed a very intense, high-energy band, with peak at 244 nm and a less intense, low-energy band, with a peak at 289 nm matching very well with the corresponding experimental absorption spectrum. The high-energy band arises from electronic transitions absorbing in the region of 210–260 nm, while the low-energy band arises from electronic transitions absorbing in the range of 280–300 nm.

The high-energy absorption band involves a multitude of electronic transitions which are due to HOMO,-1,-3,-4→LUMO,5–11,13,19 excitations. The HOMO,-1,-3,-4 are constructed from the out-of-phase combinations of Cu 3*d* AOs with ligand group orbitals mainly located on the thiolate ligand. On the other hand, the virtual MOs involved in these electronic transitions, are ligand orbitals localized on the phosphane ligand except LUMO+13 which is constructed from the out-of-phase combination of Cu 3*d* AOs with orbitals mainly located on the thiolate ligand. Thus, the high-energy band exhibits a composite electronic transition pattern involving MLCT and LLCT transitions.

The low-energy band involves electronic transitions which are due to HOMO,-3,-4→LUMO,1–3,12 excitations and therefore, this band could be assigned as a MLCT/LLCT band. However, there is also a contribution from an intraligand, IL excitation (H→L+12) as well, taking into account that LUMO+12 is entirely located on the thiolate ligand.

The calculated absorption spectrum of complex **2** showed a very intense, high-energy band, with peak at 255 nm and a less intense, low-energy band, with a peak at 297 nm in excellent agreement with the experimentally derived values (Table 1). Inspection of Figure 2 reveals that the calculated absorption spectrum of complex **2** is blue-shifted compared to that of complex **1**.

The high-energy band arises from electronic transitions in the region of 240–270 nm, while the low-energy band arises mainly from one electronic transition absorbing at 297 nm. The former involves electronic transitions which are due to HOMO,-1,-2,-3,-4→LUMO,1,4,5,6,7,10,12,13 excitations while the later involves the H-1→L+5 transition. The HOMO,-1,-2,-3,-4 are mainly located either at the Cu metal center and the thiolate ligand or entirely at the thiolate ligand. On the other hand, the unoccupied orbitals involved in the electronic transitions are all located on the phosphane ligand with the exception of LUMO+13 which is entirely located on the thiolate ligand.

Thus, the high-energy band could be assigned as a MLCT/LLCT band with a contribution from an intraligand, IL excitation (H→L+13 and H-1→L+13) as well similar to those found for complex **1**. The low-energy band could be assigned as MLCT with the charge transferred mainly from the copper metal center to the phosphane ligands.

Triplet Excited States: Emission

In order to get a deeper insight into the emission properties of complexes **1** and **2** we performed B3LYP/SDD single point energy calculations for the ground singlet, S_0 and the lowest triplet excited states, T_1 using the geometries obtained from X-ray structure analysis. It should be noticed that geometry changes upon excitation of the emissive triplet states are small for nearly all of the complexes investigated (in rigid matrices).[11] In effect optimizing both the singlet, S_0 and lowest triplet excited state, T_1 at the BP86/TZP level, the only structural change is the shortening of the Cu–S bond in the triplet state by 0.015 Å. All other geometrical parameters remain practically unchanged and very close to those found from the X-ray structural analysis.

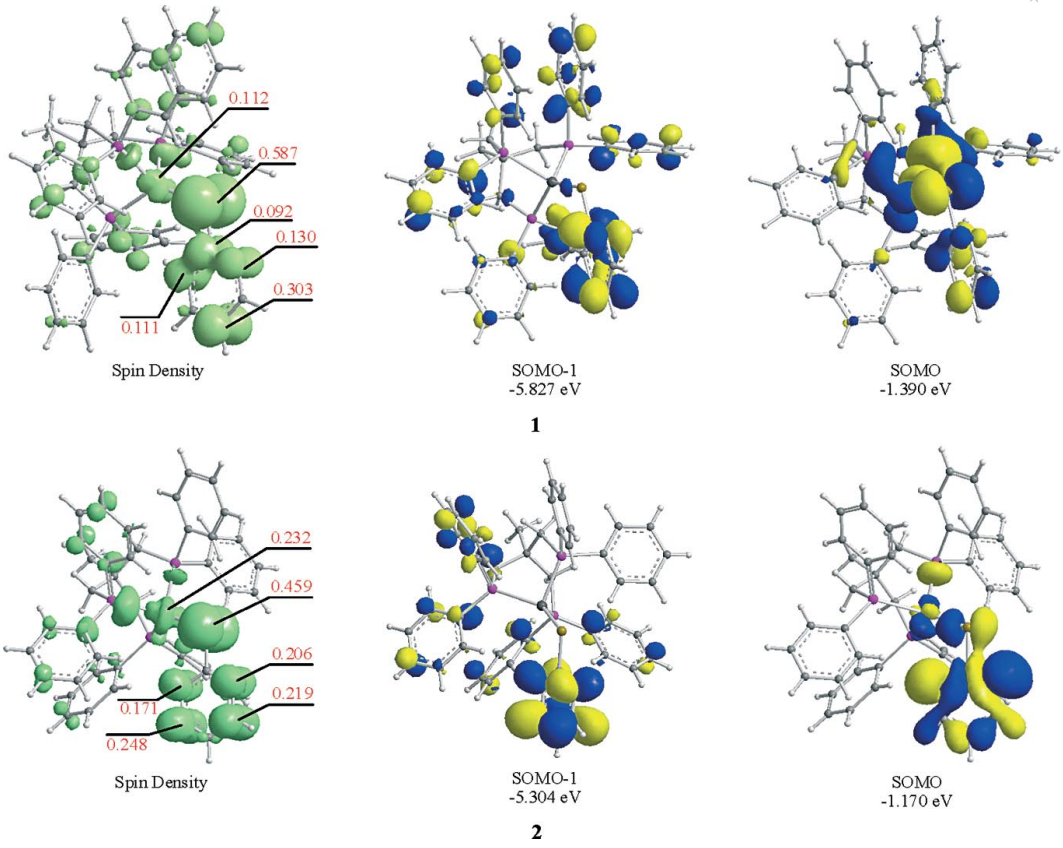

Figure 4. Spin density isosurfaces (0.002 au) along with atomic spin densities of complexes **1** and **2** and 3D contour plots of the relevant SOMOs computed at the B3LYP/SDD level.

The lengthening of the Cu–S bond in S_0 could be attributed to the accumulation of electron density on the antibonding HOMO during the de-excitation process from the lowest triplet excited state T_1 to S_0 ground state.

The spin density of complexes **1** and **2** in their lowest triplet excited state, T_1 obtained as the difference between α and β spin contributions to the total electron density, are visualized in Figure 4 along with the 3D contour plots of the Singly Occupied Molecular Orbitals (SOMOs). Inspection of Figure 4 reveals that in both **1** and **2** the spin density is delocalized over the entire nuclear framework with higher distribution on the thiolate and the phosphane ligands and lower over the copper central atom. Specifically, in complex **1** the spin density distribution amounts to 61.25% on the thiolate ligand, 33.15% on the phosphane ligand and 5.6% on the Cu metal atom while in complex **2** the total spin density distribution amounts to 65.22%, 23.18% and 11.61%, respectively. Noteworthy, in both **1** and **2** the spin density distribution is approximately accounted for by the sum of the SOMO and SOMO-1. Therefore, upon decay from T_1 to S_0, polarization of the spin will involve mainly recoupling of the electron in the SOMO (primarily distributed on the central metal atom and the thiolate ligand) with the electron residing in the SOMO-1 (primarily distributed on the thiolate and phosphane ligands), as a genuine singlet state spin density is identically zero at every point in space.

In the calculated spectrum of **1**, a spin-forbidden singlet-triplet transition around 480 nm with energy of 1.551 eV (Figure 2) corresponds to a pure H→L excitation. On the other hand, the analogous spin-forbidden singlet-triplet transition for **2** appears around 405 nm with energy of 1.850 eV. The weak spin-forbidden singlet-triplet transitions in **1** and **2** come from spin-orbit coupling. It is evident, that the intense blue-green emission in the 456–502 nm range of the emission spectra of **1** and **2** corresponds to a vertical electronic transition from the Franck Condon T_1 state to their ground S_0 state. The $T_1 \rightarrow S_0$ transition corresponds to a distant interligand charge transfer (LLCT).

X-ray Structural Investigations

The X-ray crystal structures of [Cu(κ^3-triphos)(κ^1-py2S)] (**1**) and [Cu(κ^3-triphos)(κ^1-pymt)] (**2**) are shown in Figures 5 and 6, respectively, while selected distances and angles of these complexes are compiled in Table 3.

Orange single crystals of **1** and **2** were grown from their acetonitrile/ethanol mother liquids upon slow evaporation during several days. Complexes **1** and **2** crystallize in the monoclinic space group $P2_1/c$ and in the orthorhombic space group $P2_12_12_1$ respectively, each with four discrete formula units in the unit cell. The single-crystal analysis of

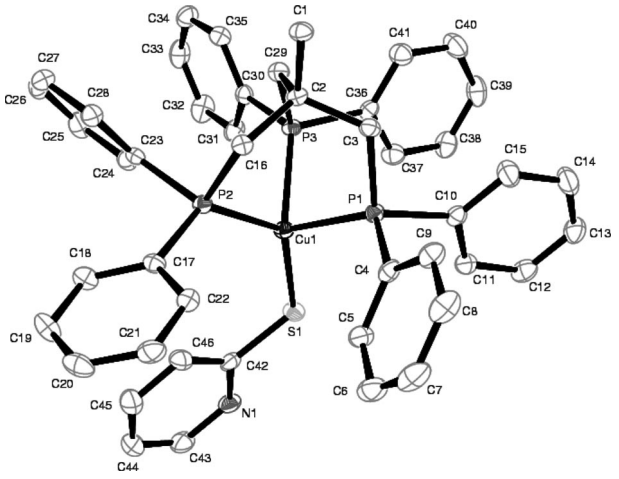

Figure 5. View of compound **1** with atom labels (disordered solvent excluded). Displacement ellipsoids are shown in the 50% probability level.

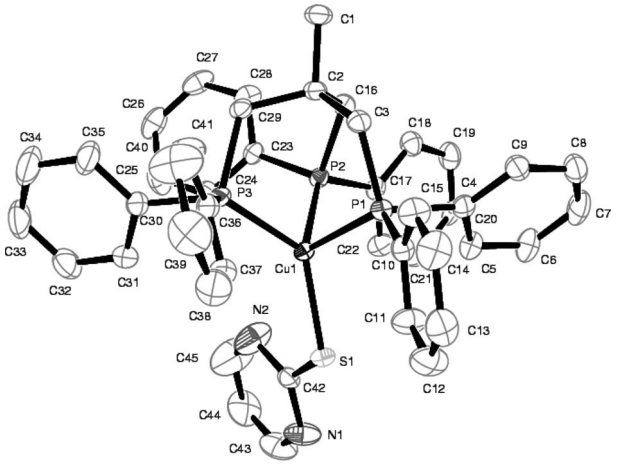

Figure 6. View of compound **2** with atom labels. Displacement ellipsoids are shown in the 50% probability level.

Table 3. Selected bond lengths [Å] and angles [°] for **1** and **2**.

Compound **1**		Compound **2**	
Cu(1)–P(1)	2.3009(6)	Cu(1)–P(1)	2.2703(7)
Cu(1)–P(2)	2.2699(6)	Cu(1)–P(2)	2.2816(7)
Cu(1)–P(3)	2.3105(6)	Cu(1)–P(3)	2.2553(7)
Cu(1)–S(1)	2.2669(6)	Cu(1)–S(1)	2.2570(7)
S(1)–C(42)	1.741(5)	S(1)–C(42)	1.717(3)
P(2)–Cu(1)–P(1)	97.96(2)	P(2)–Cu(1)–P(1)	95.36(2)
P(1)–Cu(1)–P(3)	92.61(2)	P(1)–Cu(1)–P(3)	92.65(3)
P(2)–Cu(1)–P(3)	89.45(2)	P(2)–Cu(1)–P(3)	94.41(2)
S(1)–Cu(1)–P(2)	130.84(2)	S(1)–Cu(1)–P(2)	126.58(3)
S(1)–Cu(1)–P(1)	114.00(2)	S(1)–Cu(1)–P(1)	107.66(3)
S(1)–Cu(1)–P(3)	122.49(2)	S(1)–Cu(1)–P(3)	130.48(3)
C(42)–S(1)–Cu(1)	113.29(8)	C(42)–S(1)–Cu(1)	108.44(9)

compound **1** indicates the presence of one solvent (ethanol) molecule, trapped in the crystal lattice.

As shown in the ORTEP drawings the structures of compounds **1** and **2** are quite similar having in common the highly distorted tetrahedral coordination of the copper(I) centre, which is surrounded by the P atoms of the chelating triphos and the S donor atom of the thiolate unit. Nevertheless, considering the interligand bond angles involving the central metal atom in the two structures described here, there are some notable differences. Thus, there are three markedly different P–Cu–P angles in complex **1**, ranging from 89.45(2) to 97.96(2)° whereas complex **2** is in this respect less distorted with P–Cu–P angles lying in the narrow range 92.65(3)–95.36(2)°. It should be noticed that differences within the corresponding angles found in [Cu(κ^3-triphos)Cl],[3] [Cu(κ^3-triphos)Br][4] and [PhCu(κ^3-triphos)][5] are also quite small and comparable to these observed in compound **2**. Nevertheless, such distortions within all these structures could be considered as normal due to the strain imposed by the six-membered chelate rings formed.[12]

On the other hand, the distortions within the P–Cu–S angles observed for **2**, with values differing by ca 23°, are somewhat larger than in **1**. In contrast, the individual P–Cu–X angles (X = Cl, Br, C) in the three above compounds chosen for comparison, differ only slightly from each other, thus the situation in the present two structures can be associated with the orientation of the heterocyclic ring imposed by the C(42)–S–Cu angle.

Another difference between the two structures concerns, the C(10)–C(15) and C(36)–C(41) phenyl rings, which are oriented nearly planar to each other in **1**, the dihedral angle between mean planes through these rings being 17.7(1)°. The respective stacking distance between ring centroids is 3.872(1) Å, suggesting the presence of significant π–π interactions.

The average for Cu–P bond lengths in the two compounds [2.2934(6) Å in **1** and 2.2690(7) Å in **2**] is close to the values 2.2867(17) Å and 2.2953(4) Å found in [Cu(κ^3-triphos)Cl][3] and in [Cu(κ^3-triphos)Br][4] respectively. On the other hand, each deprotonated thione ligand is bonded to the metal center in **1** and **2** with a "short" Cu–S bond length of 2.2669(6) and 2.2570(7) Å respectively, which is far from the values normally observed in other tetrahedral Cu^I complexes bearing neutral pyridine-2-thione or pyrimidine-2-thione, but also from the value of 2.302(4) Å observed for [CuBr(κ^1-py2S)(PPh_3)$_2$] bearing the heterocyclic thione ligand also in its deprotonated form.[13]

Conclusions

In the present study we have described the synthesis of five new Cu^I complexes **1**–**5** bearing phosphane and heterocyclic thiolates as ligands. X-ray structural analysis revealed that complexes **1** and **2** are quite similar having in common the highly distorted tetrahedral coordination of the copper(I) centre, which is surrounded by the P atoms of the chelating triphos and the S donor atom of the thiolate unit. The *S*-coordination mode of the thione ligand to the copper central atom is reflected in the characteristic "thioamide bands" found in the IR spectra of **1**–**5**. The absorption spectra of **1**–**5** show two intense bands with maxima in the 245–260 nm and 290–300 nm regions which according to the TD-DFT calculations are assigned as having a mixed

MLCT/LLCT character. The intense blue-green emission found in the 456–502 nm range of the emission spectra of **1** and **2** is due to a $T_1 \rightarrow S_0$ transition corresponding to a distant interligand charge transfer (LLCT) mediated by the copper central metal atom.

Experimental Section

Materials and Instrumentation: Commercially available copper(I) bromide (Merck) and 1,1,1-tris(diphenylphosphanylmethyl)ethane (Aldrich) were used as received, while the thiones (Merck or Aldrich) were re-crystallized from hot ethanol prior to their use. All the solvents were purified by respective suitable methods and allowed to stand over molecular sieves. Infra-red spectra in the region of 4000–250 cm^{-1} were obtained in KBr discs with Perkin–Elmer FT-IR Spectrum 1 spectrophotometer. Electronic absorption spectra were measured with a Perkin–Elmer–Hitachi 200 spectrophotometer while a Hitachi F-700 fluorescence spectrophotometer was used to obtain the emission spectra. Melting points were measured in open tubes with a STUART scientific instrument and are uncorrected.

Crystal Structure Determination: Single crystals suitable for crystal structure analysis were obtained by slow evaporation of acetonitrile/methanol solutions of the complexes at room temperature. X-ray diffraction data were collected on an Enraf–Nonius Kappa CCD area-detector diffractometer. The programs DENZO[14] and COLLECT[15] were used in data collection and cell refinement. Details of crystal and structure refinement are compiled in Table 4. The structures were solved using program SIR97[16] and refined with program SHELX-97.[17] Molecular plots were obtained with program ORTEP-3.[18]

CCDC-688099 (for **1**) and -688100 (for **2**) contain the supplementary crystallographic data for this paper. These data can be obtained free of charge from The Cambridge Crystallographic Data Centre via www.ccdc.cam.ac.uk/data_request/cif.

Synthesis of Complexes 1–5: To a suspension of 0.25 mmol of copper(I) bromide (35.5 mg) in 30 cm^3 of dry acetonitrile a solution of 156 mg (0.25 mmol) of 1,1,1-tris(diphenylphosphanylmethyl)ethane in 25 cm^3 of dry acetonitrile was added and the mixture was stirred at 50 °C for several hours. The resulting clear colourless solution was cooled to room temperature and then an ethanolic solution of potassium thiolate, which was prepared by treatment of 0.25 mmol of the parent thione with KOH (0.5 mL of a 0.5 M ethanolic solution) was added slowly. The resulting reaction mixture was stirred for additional two hours at 50 °C and then was filtered off and left to evaporate at ambient. The microcrystalline solid, which was deposited upon standing for several days, was filtered off and dried in vacuo. Some of the solids were recrystallized from dichloromethane.

[Cu(κ³-triphos)(py2S)]·C_2H_5OH (1): Yellow crystals (48 mg, 23%), m.p. 180–184 °C. $C_{48}H_{49}CuNOP_3S$ (844.45): calcd. C 68.31, H 5.86, N 1.66; found C 68.18, H 5.87, N 1.70. IR: $\tilde{\nu}$ = 3051 (m), 2961 (w), 1584 (m), 1571 (s), 1540 (m), 1481 (s), 1434 (vs), 1402

Table 4. Crystal data and structure refinements for [Cu(κ³-triphos)(κ¹-py2S)]·C_2H_5OH (**1**) and [Cu(κ³-triphos)(κ¹-pymt)] (**2**).

	1	**2**
Molecular formula	$C_{46}H_{43}CuNP_3S{\cdot}C_2H_5OH$	$C_{45}H_{42}CuN_2P_3S$
Formula weight	844.46	799.37
Temperature [K]	120(2)	120(2)
Wavelength [Å]	0.71073	0.71073
Crystal system	monoclinic	orthorhombic
Space group	$P2_1/c$	$P2_12_12_1$
a [Å]	9.9754(3)	9.9584(2)
b [Å]	16.6951(5)	17.6616(3)
c [Å]	25.1446(7)	22.5276(4)
α [°]	90	90
β [°]	94.8130(10)	90
γ [°]	90	90
Volume [Å³]	4172.8(2)	3962.18(13)
Z	4	4
Density (calcd.)	1.344 Mg/m^3	1.340 Mg/m^3
Absorption coefficient	0.726 mm^{-1}	0.760 mm^{-1}
F(000)	1768	1664
Crystal size [mm]	0.42 × 0.37 × 0.24	0.58 × 0.33 × 0.10
Theta range for data collection	2.93 to 27.52°	2.93 to 27.44°
Index ranges	$-12 \le h \le 12$ $-21 \le k \le 21$ $-32 \le l \le 31$	$-12 \le h \le 12$ $-22 \le k \le 22$ $-29 \le l \le 29$
Reflections collected	42623	33441
Independent reflections	9552 [R(int) = 0.0667]	9006 [R(int) = 0.0530]
Completeness	99.4% (θ = 27.52°)	99.8% (θ = 27.44°)
Data/restraints/parameters	7247/0/397	9006/0/471
Max. and min. transmission	0.8450 and 0.7501	0.9279 and 0.6670
Refinement method	full-matrix l.s. on F^2	full-matrix l.s. on F^2
Goodness-of-fit on F^2	1.030	1.027
Final R indices [$I > 2\sigma(I)$]	$R1$ = 0.0397, $wR2$ = 0.0816	$R1$ = 0.0355, $wR2$ = 0.0706
R indices (all data)	R_1 = 0.0671, $wR2$ = 0.0913	R_1 = 0.0464, $wR2$ = 0.0748
Final weighting Scheme	calcd. $w = 1/[\sigma^2(F_o^2) + (0.0315P)^2 + 2.8265P]$ where $P = (F_o^2 + 2F_c^2)/3$	calcd. $w = 1/[\sigma^2(F_o^2) + (0.0263P)^2] + 1.6912P$ where $P = (F_o^2 + 2F_c^2)/3$
Largest diff. peak and hole	0.409 and –0.467 e/Å³	0.542 and –0.345 e/Å³

(vs), 1270 (m), 1125 (vs), 1095 (vs), 1044 (m), 998 (m), 745 (s), 732 (vs), 696 (vs), 512 (vs), 493 (m) cm^{-1}. UV/Vis ($CHCl_3$): λ_{max} (logε) = 246 (4.50), 291 (4.45).

[Cu(κ³-triphos)(pymt)] (2): Pale yellow crystals (44 mg, 22%), m.p. 244 °C. $C_{45}H_{42}N_2CuP_3S$ (799.37): C 67.65, H 5.30, N 3.51; found C 67.25, H 5.34, N 3.46. IR: $\tilde{\nu}$ = 3046 (m), 2947 (w), 1585 (m), 1563 (vs), 1528 (s), 1482 (s), 1434 (vs), 1372 (vs), 1210 (m), 1179 (vs), 1094 (s), 1026 (m), 973 (m), 826 (m), 737 (vs), 696 (vs), 514 (vs), 472 (s) cm^{-1}. UV/Vis ($CHCl_3$): λ_{max} (logε) = 238 (4.16), 296 (3.85).

[Cu(κ³-triphos)(dmpymt)] (3): Pale yellow crystals (52 mg, 25%), m.p. 296 °C. $C_{47}H_{47}CuN_2P_3S$ (828.43): calcd. C 68.18, H 5.73, N 3.38; found C 67.95, H 5.56, N 3.26. IR: $\tilde{\nu}$ = 3044 (s), 2945 (m), 1582 (vs), 1528 (vs), 1480 (s), 1433 (vs), 1179 (m), 1017 (m), 991 (m), 826 (m), 735 (vs), 692 (vs), 513 (vs), 470 (s) cm^{-1}. UV/Vis ($CHCl_3$): λ_{max} (logε) = 258 (4.15), 293 (3.81).

[Cu(κ³-triphos)(tHpymt)] (3): Pale yellow powder (35.5 mg, 18%), m.p. 200–207 °C. $C_{45}H_{45}CuN_2P_3S$ (802.39): calcd. C 67.40, H 5.66, N 3.49; found C 67.00, H 5.86, N 3.32. IR: $\tilde{\nu}$ = 3042 (m), 2940 (m), 1660 (s), 1589 (vs), 1538 (s), 1481 (s), 1436 (vs), 1314 (s), 1181 (vs), 1017 (vs), 1098 (vs), 997 (m), 802 (s), 752 (vs), 739 (vs), 695 (vs), 573 (vs), 546 (vs), 503 (vs), 481 (s) cm^{-1}. UV/Vis ($CHCl_3$): λ_{max} (logε) = 263 (4.23), 298 (3.74).

[Cu(κ³-triphos)(mftzt)] (3): Pale yellow crystals (46 mg, 21%), m.p. 223 °C. $C_{45}H_{42}CuF_3N_3P_3S$ (870.37): calcd. C 62.13, H 4.87, N 4.83; found C 61.96, H 4.86, N 4.69. IR: $\tilde{\nu}$ = 3050 (s), 2952 (m), 1512 (m), 1483 (s), 1435 (vs), 1347 (vs), 1267 (s), 1185 (vs), 1026 (m), 992 (m), 827 (m), 737 (s), 693 (vs), 514 (vs), 474 (s) cm^{-1}. UV/Vis ($CHCl_3$): λ_{max} (logε) = 241 (4.44), 288 (4.23).

Computational Details: Time-dependent density functional theory (TD-DFT) calculations were performed for the singlet ground state of **1** and **2** using the geometries derived from the X-ray structural analysis of these two complexes. The SAOP (statistical averaged of orbital potentials)[19] exchange-correlation functional was used together with the TZP basis set for all atoms as implemented in the ADF 2007.01 program.[20] Calculations of the lowest 60 singlet-singlet and 60 singlet-triplet excitations at the S_0 X-ray structures of **1** and **2** were employed in order to simulate their absorption spectra. Single point energy calculations were performed at the Becke's 3-Parameter hybrid functional[21,22] combined with the Lee–Yang–Parr correlation functional[23] abbreviated as B3LYP level of density functional theory, using the basis set comprised of quasi-relativistic Stuttgart–Dresden effective small core potential,[24] for the singlet ground state, S_0 as well as for the lowest triplet excited state, T_1 of complexes **1** and **2** using the geometries obtained from their X-ray structural analysis. All single point energy calculations were done using the GAUSSIAN03 program suite.[25] The Mulliken atomic spin densities were obtained by employing Mulliken population analysis.[26]

Supporting Information (see also the footnote on the first page of this article): Excitation spectra and molecular orbitals for complexes.

Acknowledgments

We thank the Engineering and Physical Sciences Research Council (EPSRC) X-ray crystallography service at the University of Southampton for collecting the X-ray data. The authors aknowledge computer time provided by the Center for Scientific Simulations at the University of Ioannina, Greece.

[1] a) J.-C. Hierso, R. Amardeil, E. Bentabel, R. Broussier, B. Gautheron, P. Meunier, P. Kalck, *Coord. Chem. Rev.* **2003**, *236*, 143 and references therin; b) C. Bianchini, A. Meli, M. Peruzzini, F. Vizza, P. Frediani, J. A. Ramirez, *Organometallics* **1990**, *9*, 226 and references cited therein.
[2] A. B. Chaplin, P. J. Dyson, *Eur. J. Inorg. Chem.* **2007**, 4973.
[3] D. J. Fife, H. J. Mueh, C. F. Campana, *Acta Crystallogr., Sect. C* **1993**, *49*, 1714.
[4] M. I. Garcia-Seijo, P. Sevillano, R. O. Gould, D. Fernandez-Anca, M. E. Garcia-Fernandez, *Inorg. Chim. Acta* **2003**, *353*, 206.
[5] S. Gambarotta, S. Strologo, C. Floriani, A. Chiesi-Villa, C. Guastini, *Organometallics* **1984**, *3*, 1444.
[6] M. I. Bruce, N. N. Zaitseva, B. W. Skelton, N. Somers, A. H. White, *Inorg. Chim. Acta* **2007**, *360*, 681.
[7] a) P. Aslanidis, P. J. Cox, P. Karagiannidis, S. K. Hadjikakou, C. D. Antoniadis, *Eur. J. Inorg. Chem.* **2002**, 2216; b) P. Aslanidis, P. J. Cox, S. Divanidis, P. Karagiannidis, *Inorg. Chim. Acta* **2004**, *357*, 1069; c) S. K. Hadjikakou, P. Aslanidis, P. D. Akrivos, P. Karagiannidis, B. Kojic-Prodic, M. Luic, *Inorg. Chim. Acta* **1992**, *197*, 31; d) A. Kaltzoglou, P. J. Kox, P. Aslanidis, *Inorg. Chim. Acta* **2005**, *358*, 3048.
[8] V. Pawlowski, G. Knör, C. Lennartz, A. Vogler, *Eur. J. Inorg. Chem.* **2005**, 3167.
[9] C. N. R. Rao, P. Vankataraghavan, *Spectrochim. Acta* **1962**, *18*, 541.
[10] a) C. Koutal, *Coord. Chem. Rev.* **1990**, *99*, 213; b) D. R. McMillin, K. M. McNett, *Chem. Rev.* **1998**, *98*, 1201; c) P.-T. Chou, Y. Chi, *Chem. Eur. J.* **2007**, *13*, 380.
[11] H. Yersin, *Top. Curr. Chem.* **2004**, *241*, 1.
[12] D. J. Fife, W. M. Moore, K. W. Morse, *Inorg. Chem.* **1984**, *23*, 1684.
[13] P. Karagiannidis, P. Aslanidis, D. P. Kessissoglou, B. Krebs, M. Dartmann, *Inorg. Chim. Acta* **1989**, *156*, 47.
[14] Z. Otwinowski, W. Minor, in: *Macromolecular Crystallography* (Eds.: C. W. Carter Jr., R. M. Sweet), part A, vol. 276, Academic Press, New York, **1997**, pp. 307–326.
[15] R. Hooft, COLLECT Data Collection Software, Nonius BV, **1998**.
[16] A. Altomare, M. C. Burla, M. Camalli, G. L. Cascarano, C. Giacovazzo, A. Guagliardi, A. G. G. Moliterni, G. Polidori, R. Spagna, *J. Appl. Crystallogr.* **1999**, *32*, 115.
[17] G. M. Sheldrick, *SHELXL-97 Program for Crystal Strucutre Analysis*, rel. 97–2, University of Göttingen, Germany, **1997**.
[18] L. J. Farrugia, *J. Appl. Crystallogr.* **1997**, *30*, 565.
[19] *ADF2007.01* SCM, Theoretical Chemistry, Vrije Universiteit Amsterdam, The Netherlands.
[20] P. R. T. Schipper, O. V. Gritsenko, S. J. A. van Gisbergen, E. J. Baerends, *J. Chem. Phys.* **2000**, *112*, 1344–1352.
[21] A. D. Becke, *J. Chem. Phys.* **1992**, *96*, 2155.
[22] A. D. Becke, *J. Chem. Phys.* **1993**, *98*, 5648.
[23] C. Lee, W. Yang, R. G. Parr, *Phys. Rev. B* **1998**, *37*, 785.
[24] a) D. Andrae, U. Haussermann, M. Dolg, H. Stoll, H. Preuss, *Theor. Chim. Acta* **1990**, *77*, 123; b) M. Kaupp, P. v. R. Schleyer, H. Stoll, H. Preuss, *J. Chem. Phys.* **1991**, *94*,1360; c) A. Bergner, M. Dolg, W. Kuechle, H. Stoll, H. Preuss, *Mol. Phys.* **1993**, *80*, 1431; d) M. Dolg, H. Stoll, H. Preuss, R. M. Pitzer, *J. Phys. Chem.* **1993**, *97*, 5852.
[25] M. J. Frisch, G. W. Trucks, H. B. Schlegel, G. E. Scusseria, M. A. Robb, J. R. Cheeseman, J. A. Montgomery, T. Vreven, K. N. Kudin, J. C. Burant, J. M. Millam, S. S. Iyengar, J. Tomasi, V. Barone, B. Mennucci, M. Cossi, G. Scalmani, N. Rega, G. A. Petersson, H. Nakatsuji, M. Hada,M. Ehara, K. Toyota, R. Fukuda, J. Hasegawa, M. Ishida, T. Nakajima, Y. Honda, O. Kitao, H. Nakai, M. Klene, X. Li, J. E. Knox, H. P. Hratchian, J. B. Cross, C. Adamo, J. Jaramillo, R. Gomperts, R. E. Stratmann, O. Yazyev, A. J. Austin, R. Cammi, C. Pomelli, J. W. Ochterski, P. Y. Ayala, K. Morokuma, G. A. Voth, P. Salvador, J. J. Dannenberg, V. G. Zakrzewski, S. Dapprich, A. D.

Daniels, M. C. Strain, O. Farkas, D. K. Malick, A. D. Rabuck, K. Raghavachari, J. B. Foresman, J. V. Ortiz, Q. Cui, A. G. Baboul, S. Clifford, J. Cioslowski, B. B. Stefanov, G. Liu, A. Liashenko, P. Piskorz, I. Komaromi, R. L. Martin, D. J. Fox, T. Keith, M. A. Al-Laham, C. Y. Peng, A. Nanayakkara, M. Challacombe, P. M. W. Gill, B. Johnson, W. Chen, M. W. Wong, C. Gonzalez, J. A. Pople, *Gaussian 03*, rev. B.02, Gaussian, Inc. Pittsburgh P. A., **2003**.

[26] a) R. S. Mulliken, *Phys. Rev.* **1932**, *41*, 66; b) R. S. Mulliken, *J. Chem. Phys.* **1935**, *3*, 573; c) R. S. Mulliken, *J. Chem. Phys.* **1995**, *23*, 1833, 2343, 2388.

Received: July 11, 2008
Published Online: October 1, 2008

